Check for updates

(RESEARCH ARTICLE)

# Phenotypic identification of fragments as antivirals

Monika I Konaklieva [1, *], Alex Lutz [1] and Balbina J Plotkin [2]

[1] Department of Chemistry, American University, 4400 Massachusetts Ave. NW, Washington, DC, 20016-8014, USA.
[2] Department of Microbiology and Immunology, Midwestern University, Downers Grove, IL 60515.

## Abstract

While fragment-based drug discovery (FBDD), i.e., target-based approach, continues to produce candidates for research directed at drug discovery and chemical biology, a strategy increasingly being adopted is phenotypic screening, also referred to as Phenotypic Drug Discovery (PDD). Among the many therapies currently being explored, synthetic small-molecule drugs represent a prime opportunity for bringing treatments to the marketplace to meet the rising global demand for antivirals. Newer targets for antivirals are critical metabolic pathways in host cells, which viruses are known to hijack to support their replication and continued survival. Using standard synthetic techniques, a library (~50 compounds) of low molecular weight urea and amide chemotypes was developed to target virus entry. The library is based on the fragment-to-lead approach, utilizing phenotypic screen whole cell screens. The fragments based on the urea scaffold with nitrogen heterocycle, e.g., pyrimidine moiety, and the trifluoromethyl-containing amides demonstrated activity against respiratory viruses such as influenza viruses, enterovirus, and respiratory syncytial virus. These preliminary results serve as a foundation for optimizing our current fragment library to increase the potency of the next generation of compounds and to define their potential as antivirals.

**Keywords:** Antiviral; Fragment library; Phenotypic screening; Influenza viruses; Respiratory syncytial virus; Enterovirus

## 1. Introduction

Fragment-based ligand discovery (FBLD) has become a powerful approach for discovering new biologically active compounds [1]. The relatively specific binding of fragments to their molecular targets can be controlled by modulating their lipophilicity and selectivity. This focused control optimizes and streamlines the identification of fragments that exhibit higher ligand efficiency (LE) than is measured in standard high-throughput screening. There are successful examples of optimization strategies, such as LE, in the area of anti-infective lead development, through which a lead fragment is developed into a drug with clinical potential [2].

However, LE's projected utility in drug design depends on the readout mechanism used to determine activity. When minimal inhibitory concentrations MICs (antimicrobials), or compound concentrations that reduce viral replication by 50%, i.e., EC50s (antivirals), are the principal gauges of antimicrobial activity/antiviral activity, the advantage of the LE appears diminished. For adequate assessment of LE efficacy, it becomes essential after the initial hit's activity and efficacy have been optimized, to use FBLD to screen targeted microbes to identify compounds that have efficacy and safety in whole cell and mouse models screens. This mode of screening falls under the rubric of Phenotypic Drug Discovery (PDD) [3-6].

PDD is an increasingly adopted approach, while the target-based strategy of fragment-based drug discovery continues to produce drug candidates [1,6]. Although laborious, there are several advantages to phenotypic screens [7]. They

* Corresponding author: Monika I Konaklieva

include: (a) lack of bias concerning a singular protein target; (b) since target proteins are kept in their native environment, protein-protein interactions can be examined so that fragment activity is not confined to the binding events of single proteins, and; (c) alternative mechanisms, or targets, such as modulation of other classes of biomolecules (i.e., DNA, RNA, lipids, or carbohydrates) can be identified [1]. The relatively specific binding of fragments to their molecular targets can be controlled by modulating their lipophilicity and selectivity. This focused control optimizes and streamlines the identification of fragments that exhibit higher ligand efficiency (LE) than is measured in standard high-throughput screening. There are successful examples of optimization strategies, such as LE, in the area of anti-infective lead development, through which a lead fragment is developed into a drug with clinical potential [2].

However, LE's projected utility in drug design depends on the readout mechanism used to determine activity. When minimal inhibitory concentrations MICs (antimicrobials), or compound concentrations that reduce viral replication by 50%, i.e., EC50s (antivirals), are the principal gauges of antimicrobial activity/antiviral activity, the advantage of the LE appears diminished. For adequate assessment of LE efficacy, it becomes essential after the initial hit's activity and efficacy have been optimized, to use FBLD to screen targeted microbes to identify compounds that have efficacy and safety in whole cell and mouse models screens. This mode of screening falls under the rubric of Phenotypic Drug Discovery (PDD) [3-6].

PDD is an increasingly adopted approach, while the target-based strategy of fragment-based drug discovery continues to produce drug candidates [1,6]. Although laborious, there are several advantages to phenotypic screens [7]. They include: (a) lack of bias concerning a singular protein target; (b) since target proteins are kept in their native environments, successful use of PDD resulted in the therapy for hepatitis C (HCV), which identified previously unknown molecular targets [8]. PDD for drug development revolutionized HCV treatment through the development of combinations of orally available direct-acting antivirals that inhibit HCV replication and result in < 10% treatment failure. Thus, fragment libraries, in combination with phenotypic screens, can reveal sites that can be exploited to obtain clinically relevant activity and concentrations. Furthermore, phenotypic screening could have high utility in institutions with limited resources for research directed toward the identification of new antimicrobial leads at the start of an FBLD.

Currently available libraries of kinase inhibitors representing different chemotypes, including natural products, are being subjected to high-throughput screening [9-11]. We prepared our initial fragments based on two chemotypes (urea- and amide-chemotypes) that show ligand efficiency (LE) against human enzymes, including kinases. The focus of the study was on understanding what can be achieved with a chemistry-driven exploration of the space around fragments based on these two chemotypes, coupled with phenotypic antiviral testing. The synthesis of our urea- and amide-based fragments/compounds (Table 1) was intended to evaluate the presence of a heterocycle (specifically a nitrogen heterocycle) as one of the substituents on the urea- and amide moieties, in comparison to their phenyl-substituted counterparts. The latter are the subject of repurposing of reversible mammalian kinase inhibitors as antivirals. The exploration of the cyclic amide chemotype represented by a monocyclic β-lactam was intended to evaluate the effect of the lactam ring (as compared to acyclic counterparts) on the antiviral activity. The main targets of our compounds have been predicted to be mammalian kinases as per the SwissDoc (https://www.swissdock.ch/) molecular modeling program.

## 2. Material and methods

### 2.1. Chemistry

#### 2.1.1. General Instrumentation/methods.

All reagents were purchased from Sigma–Aldrich Chemical Company and used without further purification. Solvents were obtained from Fisher Scientific Company. Thin layer chromatography (TLC) was carried out using Silicycle plates with a fluorescence indicator SiliaPlate™ TLC – Glass-Backed, 250 μm, thickness F-254). Unless otherwise noted, the compounds were detected under UV light (254 nm). Products were purified by flash chromatography by gradient elution from silica gel columns (SiliaSep™ C18 (17%), particle size 40–63 μm, 60 A), and/or recrystallization. Unless stated otherwise, solutions in organic solvents were dried with anhydrous magnesium sulfate at room temperature and concentrated under vacuum conditions using rotary evaporation.

All compounds were characterized by ^{1}H and ^{13}C NMR spectra (25 °C). Spectra were obtained at 400 MHz for ^{1}H NMR and 100 MHz for ^{13}C NMR in CDCl3 or chloroform-d (Bruker 400 spectrometer, Billerica, MA). All chemical shifts (δ) are reported in parts per million (ppm) and referenced to tetramethyl silane (TMS); coupling constants (J) are reported in hertz (Hz). Abbreviations used follow: s=singlet, br=broad singlet, d=doublet, dd=double of doublet, bd=broad doublet, ddd=doublet of doublet of doublet, t=triplet, dt=doublet of triplet, q=quartet, p=pentet, m=multiplet. In most cases,

signals due to exchangeable protons were omitted. Elemental analyses were performed by Atlantic Microlab, Inc. (Norcross, GA). All compounds were 98% pure by LC-MS and NMR.
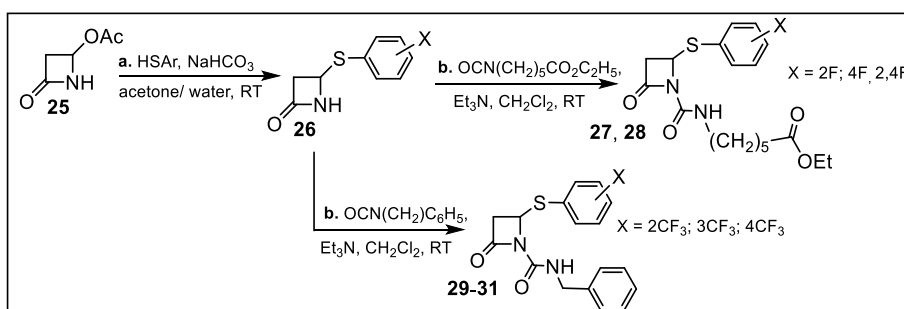
*2.1.2. Synthesis*

General procedures for the syntheses of ureas and amides used in this study. All compounds are prepared by established procedures, which are briefly described below.
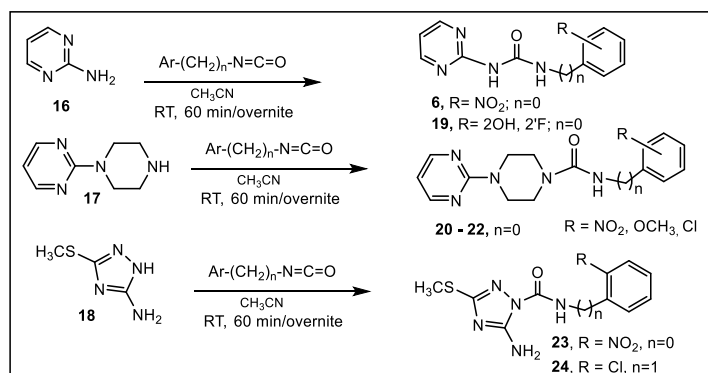


**Figure 1** Synthesis of ureas: Ureido derivatives were prepared (e.g., 6, 19-24, Table 1) from the commercially available amines 16, 17, and 18, and the corresponding commercially available isocyanates in CH2Cl2 (or CH3CN) at RT; yield 50-90% (after flash chromatography purification)

The synthetic procedure for the preparation of the carbamylated lactam derivatives was previously described [12, 13]. Briefly, to a solution of appropriate azetidine-2-one, **24** (1.7 g, 5.4 mmol) in $CH_2Cl_2$ (5 ml), were added 1.2 mol equiv. of triethylamine($Et_3N$) and 1.2 mol. equiv. of the corresponding alkyl or benzyl isocyanates (Fig. 2). The reaction was stirred at room temperature and monitored by TLC. After completion of the reaction, the solution was evaporated under reduced pressure. Further purification by flash chromatography (silica gel), Hexanes: Ethyl acetate = 2:1 gave the desired product in 40-60% yield.



**Figure 2** Synthesis of N-substituted C4 arylthio-β-lactams. a. β-Lactam 26 were prepared from the commercially available β–lactam 25 in the presence of NaHCO3 in acetone/water [12, 13]; b. β-Lactams 27, 28, and 29-31 were prepared from β-lactams 26 using alkyl isocyanate and benzyl isocyanate, respectively, in the presence of Et3N in CH2Cl2 at RT [13]

The general procedure for the preparation of acyclic amides was adapted from Cee, et al. [14] and Movassagh, et al. [15]. Briefly, amine **32** (2.45 mmol) was dissolved in $CH_2Cl_2$ (8.0 mL) and cooled to 0 °C with stirring (Fig. 3), followed by the addition of N, N-diisopropylethylamine, DIPEA (0.70 mL, 4.00 mmol). Acryloyl chloride, **33**, (0.16 mL, 2.00 mmol) was then added dropwise (Fig. 3). After 5 minutes, the reaction was warmed to room temperature and stirred for one hour to obtain acrylamide **34** (Fig. 3). To the thus prepared **34**, (0.17g, 1.00mmol) the appropriate thiophenol (0.22mL, 2.00mmol) was added and the reaction mixture was stirred at 50°C for 30 minutes to obtain amides **35-39**. The purified products were obtained in 60-75% yields after column chromatography.
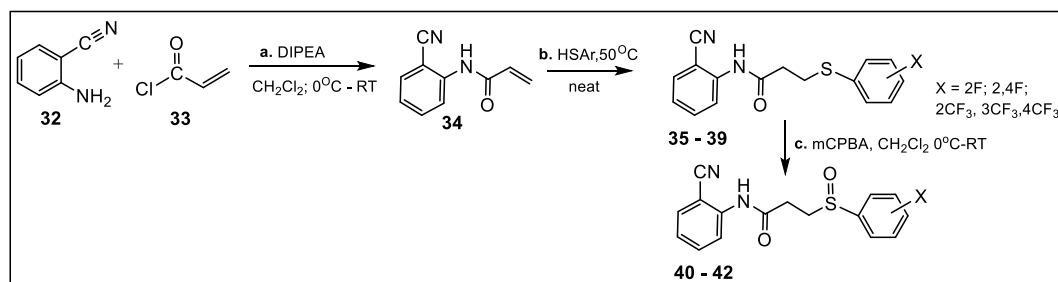
**Figure 3** Synthesis of open chain amide mimic of the β-lactams (shown above, Fig. 2): a. synthesis of acrylamide 34 from commercially available amine 32 in the presence of N, N-diisopropylethylamine, DIPEA [14]; b. preparation of amides 35-39 by addition of the appropriate aromatic thiol neat at elevated temperature [15]; c. synthesis of the sulfoxides 40-42 from the corresponding sulfides 34-38 using standard procedures (using *m*-Chloroperoxybenzoic acid, MCPBA) at 0 °C for about 10-15 minutes, then at room temperature for 45 minutes [16, 17]

## 2.2. Antiviral assays

The antiviral assays were performed through the National Institutes of Health, NIH antiviral screening program (National Institute of Allergy and Infectious Diseases, NIAID Non-Clinical Evaluation). Both antiviral activity EC50 (Half Maximal Effective Concentration) and toxicity CC50 (50% Cytotoxic Concentration) against the corresponding mammalian cell lines, as well as the corresponding SI50 (50% Selectivity Index) were determined. The ratio activity/toxicity is expressed by $SI_{50}$, where a compound is defined as a promising antiviral candidate with a $SI_{50} > 10$. It is generally accepted that compounds with $SI_{50} \leq 1$ are considered toxic, $SI_{50} \geq 5$ as acceptable, and $\geq 10$ as selective bioactive compounds [18-21].

Briefly, the antiviral activity ($EC_{50}$) of the synthesized compounds was tested at a drug range of 0.1-100 mg/mL with the corresponding drug as a control at 1-1000mg/mL concentrations. Each antiviral activity was determined by the cytotoxicity (cytopathic effect/toxicity) assays ($CC_{50}$ determination) (Visual; Promega) and validated by the Neutral Red (Millipore-Sigma) Cytopathic effect/Toxicity kits as previously described [22]. In addition, the compounds presented in Table 1 were evaluated by the standard virus yield reduction, i.e., secondary VYR assay [22].

The antiviral activity ($EC_{50}$) of the compounds from our library was determined in duplicates at 0.1-100 mM drug concentrations with the following controls: EIDD 1931 for chikungunya virus; infergen for dengue virus and yellow fever virus; pirodavir for enterovirus; cidofovir for adenovirus; acyclovir for herpes simplex virus 1; ganciclovir for human cytomegalovirus (HCMV); M128533 for MERS Corona V; 2'-difluoro-2' Deoxycytidine for measles virus; ribavirin for all the influenza viruses (IVs), respiratory syncytial virus (RSV), Rift Valley Fever Virus (RVFV) and Tacaribe Virus; enviroxime for poliovirus-1. The cytotoxicity (Cytopathic effect/Toxicity) assays ($CC_{50}$ determination) used were the Visual (Promega) and Neutral Red (Millipore-Sigma) Cytopathic effect/Toxicity kits. These assays were used synchronously for all the influenza viruses (IVs) and respiratory syncytial virus (RSV), as well as chikungunya virus, dengue virus 2, MERS Coronavirus, measles, Rift Valley Fever virus, Tacaribe virus, poliovirus-1 and yellow fever virus. CellTiter-Glo (Promega) Cytopathic effect/Toxicity assay was used for adenovirus.

## 3. Results and discussion

### 3.1. Amide and urea chemotypes for the fragment library

For this study, a library of ~50 compounds was prepared based on the amide- and urea chemotypes that consisted mostly of fragments of MW <300, with a dozen compounds having MW up to 400. Several ureas (Table 1) and amides (Table 1) have been identified through these screening efforts. The antiviral potential of our compound library was evaluated using the following viruses: influenza A viruses (IAV) (H1N1, H3N2; H5N1), influenza B virus (IBV); respiratory syncytial virus (RSV); chikungunya virus; dengue virus; enterovirus; MERS-Corona virus; measles virus; Rift Valley Fever Virus, (RVF); Tacaribe virus; yellow fever virus; adenovirus; herpes simplex virus 1 (HSV); poliovirus-1 and, human cytomegalovirus (HCMV). From the ~50-compound library, several compounds demonstrated antiviral activity. The structures of those with acceptable and promising activity (12 compounds) are shown in Table 1.

## 3.2. Rationale for the synthesis of urea-based fragments reported in the literature (other than the FDA-approved antiviral ureas)

A heterocycle directly attached to the urea's nitrogen as an antiviral is rarely reported in the literature [23-30]. The synthesis of our urea-based fragments was intended to evaluate the presence of a heterocycle (specifically a nitrogen heterocycle) as one of the substituents on one of the urea moiety nitrogen atoms, as compared to their phenyl-substituted counterparts. The majority of the most promising compounds against different viruses, based on both $EC_{50}$ and $SI_{50}$ values, contain either fluoro- or trifluoromethyl groups from both urea and amide classes (19, 36, 38, and 41, Table 1).

Compounds from both urea and amide chemotypes demonstrated the best activity against respiratory viruses. Representatives of the amide chemotype, having fluorinated phenyl ring (28 and 36, Table 1), demonstrated activity against dengue virus 2, with the lactam scaffold (28, Table 1) having better activity as compared with its acyclic amide counterpart (36, Table 1). The two amides (38 and 41, Table 1), and to a lesser extent β-lactam 30 (Table 1), which contain trifluoromethylated phenyl substituent, demonstrated very good activity against H1N1 and RSV.

All heterocyclic ureas demonstrated activity against respiratory viruses, IVs, and RSV, except urea 19 (Table 1), whose main activity was confined to enterovirus, as well as adenovirus, herpes simplex 1, and HCMV. Of the ureas, urea 6a (Table 1) demonstrated activity against all four influenza viruses. To the best of our knowledge, antiviral activities, other than activity against Coxsackie A21 virus infections in mice [23], for the 2-pyrimidylureas have not been reported in the literature, although the pyrimidine ring is present in several antiviral compounds [31-36].

Amides 36 and 38 (Table 1) were synthesized to have a similarly fluorinated thiophenyl substituent to lactams 28 and 30 (Table 1), i.e., the thiophenyl group had the same distance to the carbonyl carbon as in lactams 28 and 30 (Table 1). The rationale for this design was to evaluate the importance of cyclic (28 and 30, Table 1) vs. acyclic amides (28 and 30, Table 1). Preparation of the sulfoxide 41 (Table 1) was inspired by the "classic" bicyclic β-lactams reported as inhibitors of the SARS-CoV-2 viral cysteine protease (Mpro) [16,17]. We were interested in this design since it would assist in evaluating the effect of the oxidation state of the sulfur atom on the activity of these amides. We have found no reports of compounds with structural similarity to our amides with antiviral activity.

The fragment-based drug discovery is typically used against molecular targets [37]. We hypothesized that fragments that are small enough to bind multiple sites are more likely to be accepted as substrate analogs of a wider set of enzymes, which could lead to preventing viral replication. "Multitarget drug discovery is a more complete paradigm than its one-drug-to-one target counterpart because finding multitarget inhibitors will allow for obtaining information about target preferences and selectivity, thus providing insights for the design of selective inhibitors" Kleandrova, V. et al, [38], and demonstrated by the *in vitro* studies of the potential of MP1032, an immune-modulating drug, for treating COVID-19 [39]. The current study is directed to assess the *in vitro* antiviral activity of the compounds we synthesized. This work represents a foundational study showing the utility of these low molecular weight compounds as potential antivirals. Further studies to refine activity, lower toxicity, and prevent off-target effects are part of the next phase of the study.

The two main scaffolds used in our fragment libraries are (i) amides and (ii) aryl ureas. In addition to the repurposing of FDA-approved drugs as antivirals, amides and ureas have been demonstrated to inhibit a multitude of viral protein enzymatic activities involved in viral replication [40]. Furthermore, targeting shared steps in viral entry, replication, and egress has distinct advantages in that it has an increased likelihood that broad-spectrum antivirals will be identified.
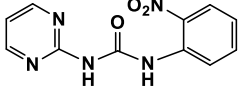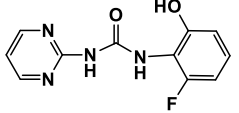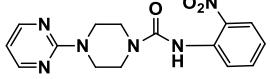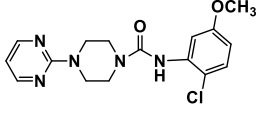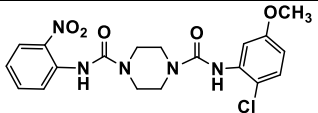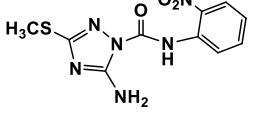
Mammalian protein kinases are one set of proteins receiving significant attention as putative targets for antiviral agents. These proteins are well-characterized and are established as druggable host factors. Many of the inhibitors of human protein kinases are currently being repurposed as antimicrobials and antivirals.
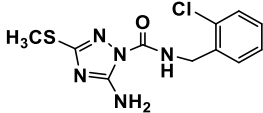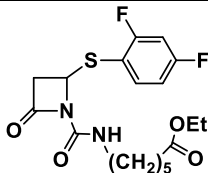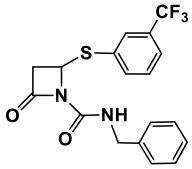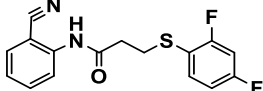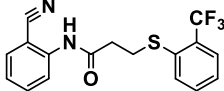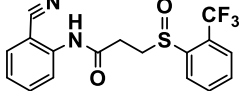
In this study, the mixture of fragments and compounds with molecular weights in between those of fragments and typically used small molecules as drugs was envisioned to allow the coverage of an expanded pharmacology space, as has been reported earlier [6].

Since we built the compound library based on two main chemotypes that are at the core of kinase inhibition, we used the molecular modeling program SwissDoc (https://www.swissdock.ch/) to obtain information about the physicochemical properties of these compounds, their drug-likeliness, and their potential molecular targets.

**Table 1** The most promising fragments/compounds as antivirals from our library. EC50 - compound concentration that reduces viral replication by 50%; CC50 - compound concentration that reduces cell viability by 50%; SI50 = CC50/EC50.

Toxicity in all tests is measured by Visual (Cytopathic effect/Toxicity) and Neutral Red (Cytopathic effect/Toxicity), and secondary VYR assay. Compounds from our compound library (CL)

| Compound UREAS | Virus | Assay system/ Control µg/mL | Antiviral activity $EC_{50}$/ µg/mL | Cytotox/ Cell line and $CC_{50}$/ µg/mL | $SI_{50}$ valu $CC_{50}$/ $EC_{50}$ | Anti-viral Ref. |
|---|---|---|---|---|---|---|
| **6a** MW 259.23 LogP 0.74 | IAV/ H1N1 H3N2 H5N1 IBV | MDCK Ribavirin $EC_{50}$ 3.6 $CC_{50}$>1000 | 0.53 4.9 32 3.2 | 3.8 34 56 56 | 7.2 6.9 1.8 18 | [22] |
| **19** MW 248.22 LogP 0.86 | enterovir.71 adenovirus herpes simplex 1 HCMV | Vero 76 Pirodavir $EC_{50}$ 0.039 CC50 >10 HFF Cidofovir $EC_{50}$ 3.83 $CC_{50}$>150 HFF Acyclovir $EC_{50}$ 2.16 $CC_{50}$>150 HFF Ganciclovir $EC_{50}$ 0.98 $CC_{50}$>150 | 5.6 6.0 30 6.0 | >100 16.89 58 19 | 18 <3 <2 <3 | CL |
| **20** MW 328 LogP 0.75 | IAV/ H3N2 RSV | MDCK Ribavirin $EC_{50}$ 3.6 $CC_{50}$>1000 MA-104 Ribavirin $EC_{50}$ 8.2 $CC_{50}$>145 | 48 21 | >100 100 | 2.1 4.8 | [33, 34, 35] |
| **21** MW 347.80 LogP 1.92 | RSV | MA-104 Ribavirin $EC_{50}$ 8.2 $CC_{50}$>145 | 5.6 | 32 | 5.7 | 33, 34, 35] |
| **22** MW 433 LogP 2.55 | IAV/ H1N1 RSV | MDCK Ribavirin $EC_{50}$ 3.6 $CC_{50}$>1000 $EC_{50}$ 3.6 $CC_{50}$>1000 | 35 45 | >100 >100 | 2.9 2.2 | CL |
| **23** MW 294.29/ LogP 1.124 | IAV/ H1N1 | MDCK Ribavirin $EC_{50}$ 3.6 $CC_{50}$>1000 | 43 | 46 | 1.1 | CL |

| | IAV/ H1N1 | MDCK Ribavirin $EC_{50}$ 3.6 $CC_{50}$>1000 | 2 | 12 | 6 | CL |
|---|---|---|---|---|---|---|
| **24** MW 297.76 LogP 2.24 | | | | | | |

| Compound | Virus | Assay system/ Control µg/mL | Antiviral activity $EC_{50}$/ µg/mL | Cytotox/Cell line and $CC_{50}$/ µg/mL | **SI** valu$C_{50}$/E$C_{50}$ | Antiviral Ref. |
|---|---|---|---|---|---|---|
| CARBAMYLATED β-LACTAMS | | | | | | |
| **28** MW 382.14 LogP 3.1 | dengue virus 2 | Huh7 Infergen $EC_{50}$ <0.00001 $CC_{50}$ >0.01 | 2.8 | 16 | 5.7 | CL |
| **30** MW 380.4 LogP 4.33 | IAV/ H1N1 | MDCK Ribavirin $EC_{50}$ 3.6 $CC_{50}$>1000 | 4.6 | 24 | 5.2 | CL |
| AMIDES | | | | | | |
| **36** MW 318.34 LogP 3.63 | dengue virus 2 | Huh7 Infergen $EC_{50}$ <0.00001 $CC_{50}$ >0.01 | 28 | 42 | 1.5 | CL |
| **38** MW 350.07 LogP 4.24 | IAV/ H1N1 RSV | MDCK Ribavirin $EC_{50}$ 3.6 $CC_{50}$>1000 | 25 3.7 | >100 50 | 2.9 14 | CL |
| **41** MW 366.36 LogP 2.63 | IAV/ H1N1 H3N2 IBV(Brisb.) RSV | MDCK Ribavirin $EC_{50}$ 3.6 $CC_{50}$>1000 MA-104 Ribavirin $EC_{50}$ 8.2 $CC_{50}$>145 | 11 63 61 3.7 | >100 >100 >100 >50 | 9.1 1.6 1.6 14 | CL |

The predicted molecular targets by SwissDoc with the highest probability for our ureas (Table 1) are kinases and Family A G-Protein coupled receptors (GPCR-A), which are both host targets hijacked by viruses, including IVs [41-43]. The predicted molecular targets by SwissDoc with the highest probability for the thiophenyl-containing amides (Table 1) are kinases, regardless of the type of fluorination of the phenyl ring. The molecular targets of the amides with oxidized thiophenyl group (e.g., 37, Table 1) are predicted with the highest probability to be kinases, followed by histone deacetylases (HDACs), which also play a key role in viral replication [44, 45].

The compounds were tested in several groups over several months. Some viruses are more difficult to grow than others; thus, not all viruses were available for testing at the same time for a specific group of compounds. The cut-off for compounds is based on $SI_{50}$ values: compounds demonstrating $SI_{50} \geq 10$ for at least one virus are considered promising for further investigation. These include compounds 6a, 19, 38, and 41 (Table 1). In addition, those with structural similarity to the latter four compounds, but differing in their substituents, with $SI_{50}$ values placing them in the category of acceptable activity, are also included in Table 1 for illustrative purposes.

The synthesis of our urea-based fragments (Table 1) was intended to evaluate the presence of a heterocycle (specifically, a nitrogen heterocycle) as one of the substituents on one of the urea moiety nitrogen atoms, as compared to their phenyl-substituted counterparts. Since both ureas from our library that have demonstrated a promising antiviral activity contain a pyrimidine moiety (6a and 19, Table 1), the latter will be present in the majority of the next generation of urea-based fragments. The effect of the pyrimidine moiety on the activity appears to be due mainly, but not limited, to the low LogP (6a, 19-22, Table 1, having the lowest of all compounds tested) of these urea derivatives. The small size of the fragments, especially those with high hydrophilicity, presents advantages such as higher cell-membrane permeability.

The structures of our urea-based fragments (Table 1) with the best antiviral activity are characterized by (i) the presence of electron-donating (EDG) groups on the phenyl substituent of fragment 19 (Table 1) that leads to its activity against enterovirus; (ii) the presence of a powerful electron-withdrawing group (EWG) in fragment 6a, (Table 1) which broadly "shifts" the activity towards all the influenza viruses tested, with the best activity against IVB-Brisbane. The antiviral activity of urea 6a (Table 1) against the four influenza viruses is comparable to that of ribavirin; however, the SI value of ribavirin is considerably higher than that of 6a (Table 1). The structures of our urea fragments with anti-IV activity differ from the human kinase inhibitors in clinical use as cancer agents that also have demonstrated activity against IAV, i.e., regorafenib, by having a heterocycle as one of the substituents, such as 2-amino-pyrimidine, 6a (Table 1) or 3-amino-5-methylthio-1H-1,2,4-triazole (AMT), 23 and 24 (Table 1) on the urea moiety [11]. The activity of urea 6a (Table 1), specifically against IVs, distinguishes it from the pyrimidine-, as well as other heterocycle-containing compounds reported in the literature [24]. It is interesting to note that fragment 19 (Table 1) has demonstrated activity against similar viruses as those described in the literature for the piperazine-2-one derivatives, as well as pyrimidine amides, i.e., adenovirus and HCMV [23, 34, 35]. Fragment 19 (Table 1) demonstrated the best activity against enterovirus. In summary, all representatives of the urea class, except 19 (Table 1), demonstrated activity against IVs and RSV, with various degrees of activity/toxicity.

Phenotypic evaluation of the synthesized amides, i.e., structure-activity relationship (SAR) (Table 1), as antivirals point to the following): (i) presence of a trifluoromethyl group in the thiophenyl substituent (as sulfide or sulfoxide) in the acyclic amide (compounds 38 and 41 leads to good activity against RSV and IAV H1N1, as well as to the activity of lactam 30, Table 1) against H1N1. The somewhat lower activity of lactam 30 as compared to amide 38 (Table 1) could be at least partially attributed to the higher LogP as compared to the acyclic counterpart (38, Table 1). The three amides with trifluoromethylated thiophenyl substituent - lactam 30, thioether 38, and sulfoxide 41 (the latter tested as a mixture of diastereomers, Table 1) demonstrated very good activity against H1N1 and RSV. (ii) The presence of a fluorinated thiophenyl substituent appears to be a necessary structural feature for the acyclic amides and β-lactams to have activity against dengue virus (compounds 28 and 36, Table 1). Since the activity/SI of the acyclic and cyclic amides active against dengue virus 2 is very similar, further synthetic efforts will be directed toward the improvement of the activity of the acyclic amides such as 36 (Table 1). In summary, the amides appear to have promising activity against IVs, RSV, and dengue virus, and lower toxicity as compared to the similarly substituted ureas. Further optimization of both classes toward lowering toxicity, however, should be attempted.

As mentioned above, the majority of FBDD evaluate the binding of the fragments to a known drug target. Due to the usually weak binding of the fragments to their molecular targets, it has been assumed that their binding to a given target would not prove detectable by a phenotypic screen (whole cell screen), unless the fragments are used in high concentrations, e.g., > 100 mM [46]. The high fragment concentration needed to overcome the drawbacks of their weak binding, coupled with the lower sensitivity of the whole-cell assays, would lead to artifacts. This assumption that a much higher fragment concentration is needed for elucidating a reliable SAR from a whole-cell assay has been recently

challenged by identifying fragments that exhibit favorable antimicrobial and antiviral drug properties in whole-cell screens and mouse models [3-5, 6]. Inspired by these reports, we used phenotypic screens to evaluate the potential of our small library, made of predominantly fragments, against a variety of viruses (using a variety of cell lines required by the given virus type).

## 4. Conclusion

We designed, synthesized, and tested C4-arylthio, N1-carbamyl β-lactams, and amides with the S-atom of the arythio-substituent in an equal distance to the carbonyl carbon as is the arylthio-β-lactams. The development of an anti-IV library of compounds is based on the presence of functionalities, such as trifluoromethylated aryl and pyrimidyl moieties with varying other substituents that can be introduced in both chemotypes, and they have been evaluated as antivirals. The fragments based on the urea scaffold and the trifluoromethyl-containing amides have demonstrated activity against respiratory viruses such as IVs and RSV. The fragments from the urea class, specifically those having a heterocycle such as a 2-amino-pyrimidine or 3-amino-5-methylthio-1H-1,2,4-triazole directly attached to the urea moiety, have activity against IV and Enterovirus. The specific activity against enterovirus of one of the ureas, as compared to the activity of the other compounds of the urea chemotype against IV, appears to be related to the difference in the substitution on the phenyl substituent. Both the acyclic amides and β-lactams, with difluoro-substituted thiophenyls, have demonstrated modest activity against the dengue virus 2.

Our approach is to choose scaffolds that demonstrate activity against host proteins used by viruses for their entry and proliferation in the host, so it is virus-directed toward host proteins. There is an indication stemming from the presence of the urea scaffold and the predicted by SwissDoc targets that the compounds from our library appear to be targeting host enzymes, rather than viral ones. Future studies in target identification are indeed needed. Our current priority, however, is improving the drug likeness (the ADME/Absorption, distribution, metabolism, and excretion properties of a compound that make it suitable as a potential drug) of our compounds. The second generation of compounds should expand our understanding of SAR, which will allow for more defined efforts toward obtaining a compound(s) with improved antiviral activity.

These compounds are suitable candidates for lead optimization and target identification studies. This work also adds to the few existing reports on the utility of phenotypic screens in determining fragments' potential as antivirals, with the added benefit of attempting to modulate/inhibit the host's molecular targets. The development of effective, especially pan-antiviral compounds with low toxicity to the host, together with high-throughput screening, will most likely lead to a faster discovery of agents as antivirals. Our results suggest that phenotypic screens can be useful in determining the activity and toxicity of fragments, providing the opportunity to "correct" the toxicity at the early stages of the fragments' further optimization.

## Compliance with ethical standards

### *Disclosure of conflict of interest*

The authors declare no conflicts of interest

## References

[1]  Woodhead, A. J.; Erlanson, D. A.; de Esch, I. J. P.; Holvey, R. S.; Jahnke, W.; Pathuri, P. Fragment-to-Lead Medicinal Chemistry Publications in 2022. J. Med. Chem. 2024, 67, 2287-2304.

[2] Basarab, G.S.; Hill, P.J.; Garner, C.E.; Hull, K.; Green, O.; Sherer, B.A.; Dangel, P.B.; Manchester, J.I.; Bist, S.; Hauck, S.; Zhou, F.; Uria-Nickelsen, M.; Illingworth, R.; Alm, R.; Rooney, M.; Eakin, A. E. Optimization of Pyrrolamide Topoisomerase II Inhibitors toward Identification of an Antibacterial Clinical Candidate (AZD5099). J. Med. Chem. 2014, 57, 6060–6082.

[3] Moreira, W.; Lim, J.J.; Yeo, S.Y.; Ramanujulu, P.M.; Dymock, B.W.; Dick, T. Fragment-Based Whole Cell Screen Delivers Hits against M. tuberculosis and Non-tuberculous Mycobacteria. Front Microbiol. 2016, 7, 1392.

[4] Negatu, D.A.; Liu, J.J.J.; Zimmerman, M.; Kaya, F.; Dartois, V.; Aldrich, C.C.; Gengenbacher, M.; Dick, T. Whole-Cell Screen of Fragment Library Identifies Gut Microbiota Metabolite Indole Propionic Acid as Antitubercular. Antimicrob. Agents Chemother. 2018, 62, e01571-17.

[5] Ayotte, Y.; Bilodeau, F.; Descoteaux, A.; LaPlante, S.R. Fragment-Based Phenotypic Lead Discovery: Cell-Based Assay to Target Leishmaniasis. ChemMedChem 2018, 13, 1377–1386.

[6] Ayotte, Y.; Bernet, E.; Bilodeau, F.; Cimino, M.; Gagnon, D.; Lebughe, M.; Mistretta, M.; Ogadinma, P.; Ouali, S-L.; Sow, A. A.; Chatel-Chaix, L.; Descoteaux, A.; Manina, G.; Richard, D.; Veyrier, F.; LaPlante, S. R. Fragment-Based Phenotypic Lead Discovery To Identify New Drug Seeds That Target Infectious Diseases. ACS Chem. Biol. 2021, 16, 2158 – 2163.

[7] Vincent, F.; Nueda, A.; Lee, J.; Schenone, M.; Prunotto, M.; Mercola, M. Phenotypic drug discovery: recent successes, lessons learned and new directions. Nat Rev Drug Discov. 2022, 21, 899-914.

[8] Lemm, J. A.; O'Boyle, D. 2nd; Liu, M.; Nower, P.T.; Colonno, R.; Deshpande, M.S.; Snyder, L.B; Martin, S.W.; St. Laurent, D.R.; Serrano-Wu, M.H.; Romine, J.L.; Meanwell, N.A.; Gao, M. Identification of hepatitis C virus NS5A inhibitors. J. Virol. 2010, 84, 482–491.

[9] Meineke, R.; Rimmelzwaan, G. F.; Elbahesh, H. Influenza Virus Infections and Cellular Kinases. Viruses, 2019, 11, 171.

[10] Mondal, A.; Dawson, A. R.; Potts, G. K.; Freiberger, E. C.; Baker, S. F.; Moser, L. A.; Bernard, K. A.; Coon, J. J.; Mehle, A. Influenza virus recruits host protein kinase C to control assembly and activity of its replication machinery. eLife 2017, 6, e26910.

[11] Raghuvanshi, R.; Bharate, S. B. Recent Developments in the Use of Kinase Inhibitors for Management of Viral Infections. J. Med. Chem. 2022, 65, 893–921.

[12] Mulchande, J.; Martins, L.; Moreira, R.; Archer, M.; Oliveira, T.F.; Iley, J. The Efficiency of C-4 substituents in activating the β-lactam scaffold towards serine proteases and hydroxide ion. Org Biomol Chem. 2007, 5, 2617–2626.

[13] Kuskovsky, R., Lloyd, D., Arora, K., Plotkin, B., Green, J., Boshoff, H., Barry, C., Deschamps, J., Konaklieva, M. I. C4-Phenylthio β-lactams: Effect of the Chirality of the β-Lactam Ring on Antimicrobial Activity. Bioorganic and Medicinal Chemistry 2019, 27, 115050.

[14] Cee, V. J.; Volak, L. P.; Chen, Y.; Bartberger, M. D.; Tegley, C.; Arvedson, T.; McCarter, J.; Tasker, A. S.; Fotsch, C., Systematic Study of the Glutathione (GSH) Reactivity of N-Arylacrylamides: 1. Effects of Aryl Substitution. Journal of Medicinal Chemistry 2015, 58, 9171-9178.

[15] Movassagh, B.; Shaygan, P., Michael addition of thiols to α,β-unsaturated carbonyl compounds under solvent-free conditions. 2006, ARKIVOC 2006(12)DOI:10.3998/ark.5550190.0007.c15

[16] Malla, T. R., Tumber, A., John, T., Brewitz, L., Strain-Damerell, C., Owen, C. D., Schofield, C. J. Mass spectrometry reveals the potential of β-lactams as SARS-CoV-2 M pro inhibitors. Chemical Communications 2021, 57, 1430-1433.

[17] Malla, T. R.; Brewitz, L.; Muntean, D-G.; Aslam, H.; Owen, C. D.; Salah, E.; Tumber, A.; Lukacik, P.; Strain-Damerell, C.; Mikolajek, H.; Walsh, M. A.; Schofield, C. J. Penicillin Derivatives Inhibit the SARS-CoV-2 Main Protease by Reaction with Its Nucleophilic Cysteine. J. Med. Chem. 2022, 65, 7682-7696.

[18] Awouafack, M.D.; McGaw, L.J.; Gottfried, S.; Mbouangouere, R.; Tane, P.; Spiteller, M.; Eloff, J.N. Antimicrobial activity and cytotoxicity of the ethanol extract, fractions and eight compounds isolated from Eriosema robustum (Fabaceae). BMC Complement. Altern. Med. 2013, 13, 289.

[19] Indrayanto, G.; Putra, G.S.; Suhud, F. Chapter Six—Validation of In-Vitro Bioassay Methods: Application in Herbal Drug Research. In Profiles of Drug Substances, Excipients and Related Methodology; Al-Majed, A.A., Ed.; Academic Press: Cambridge, MA, USA, 2021; Volume 46, pp. 273–307. ISSN 1871-5125. ISBN 9780128241271.

[20] Indrayanto, G. The importance of method validation in herbal drug research. J. Pharm. Biomed. Anal. 2022, 214, 114735

[21] Maldonado, S.; Fuentes, P.; Bernabeu, E.; Bertera, F.; Opezzo, J.; Lagomarsino, E.; Lee, H.J.; Martínez Rodríguez, F.; Choi, M.R.; Salgueiro, M.J.; et al. Efavirenz Repurposing Challenges: A Novel Nanomicelle-Based Antiviral Therapy Against Mosquito-Borne Flaviviruses. Pharmaceutics 2025, 17, 24

[22] Sparrow, K. J.; Shrestha, R.; Wood, J. M.; Clinch, K.; Brett, B. L.; Wang, H.; Gowen, B. B.; Julander, J. G.; Tarbet, E. B.; McSweeney, A. M.; Ward, V. K.; Evans, G. B.; Harris, L. D. ACS Medicinal Chemistry Letters 2023, 14, 506-513.

[23] Paget, C. J.; Kisner, K.; Stone, R. L.; DeLong, D. C. Heterocyclic substituted ureas. II. Immunosuppressive and antiviral activity of benzothiazole- and benzoxazoleureas. J. Med. Chem. 1969, 12, 1016-8.

[24] Xu, H.; Cheng, M.; Chi, X. Liu, X.; Zhou, J.; Lin, T.; Yang, W. High-Throughput Screening Identifies Mixed-Lineage Kinase 3 as a Key Host Regulatory Factor in Zika Virus Infection. J Virol. 2019, 93, e00758-19.

[25] Voss, S.; Nitsche, C. Inhibitors of the Zika virus protease NS2B-NS3. Bioorg. Med. Chem. Lett. 2020, 30, 126965.

[26] Longshaw, A.I.; Fordyce, E.A.F.; Onions, S.T.; King-Underwood, J.; Venable, J.D. Preparation of Aromatic Heterocyclic Compounds as p38 MAP Kinase Inhibitors with Antiinflammatory Activity. WO Patent Application No. 2015121444, 20 August 2015

[27] King-Underwood, J.; Murray, P.J.; Williams, J.G.; Buck, I.; Onions, S.T. Preparation of Pyrazolyl Naphthyl Ureas as p38 MAP Kinase Inhibitors. WO Patent Application No. 2011124930, 13 October 2011

[28] King-Underwood, J.; Ito, K.; Strong, P.; Rapeport, W.G.; Charron, C.E.; Murray, P.J.; Williams, J.G.; Onions, S.T. 1-(5-Pyrazolyl)-3-(1-naphthyl)ureas as Enzyme Inhibitors and their Preparation, Pharmaceutical Compositions and Use in the Treatment of Inflammatory Disorders. WO Patent Application No. 2011124923, 13 October 2011.

[29] Ito, K.; Strong, P.; Rapeport, W.G.; Murray, P.J.; King-Underwood, J.; Williams, J.G.; Onions, S.T.; Joly, K.; Charron, C.E. Preparation of Pyrazolyl Ureas as p38 MAP Kinase Inhibitors. WO Patent Application No. 2010067130, 21 April 2011

[30] Murray, P.J.; Onions, S.T.; Williams, J.G.; Joly, K. Preparation of Pyrido[2,3-b]pyrazine Compounds for Use in Drug Formulations for Treating Inflammation, Respiratory Disorders, and Viral Infections. WO Patent Application No. 2011158044 A2 20111222, 22 December 2011.

[31] Kang, D.; Ruiz, F.X.; Sun, Y.; Feng, D.; Jing, L.; Wang, Z.; Zhang, T.; Gao, S.; Sun, L.; De Clercq, E.; Pannecouque, C.; Arnold, E.; Zhan, P.; Liu, X. 2,4,5-Trisubsituted pyrimidines as potent HIV-1 NNRTIs: Rational design, synthesis, activity evaluation, and crystallographic studies. J. Med. Chem. 2021, 64, 4239–4256.

[32] Jiang, X.; Huang, B.; Rumrill, S.; Pople, D.; Zalloum, W.A.; Kang, D.; Zhao, F.; Ji, X.; Gao, Z.; Hu, L.; Wang, Z.; Xie, M.; De Clercq, E.; Ruiz, F.X.; Arnold, E.; Pannecouque, C.; Liu, X.; Zhan, P.Discovery of 4-diarylpyrimidine derivatives bearing piperazine sulfonyl as potent HIV-1 nonnucleoside reverse transcriptase inhibitors. Commun.Chem. 2023, 6, 83.

[33] Wang, S.; Ying, Z.; Huang, Y.; Li, Y.; Hu, M.; Kang, K.; Want, H.; Shao, J.;Wu, G.; Yu, Y.; Du, Y.; Chen, W. Synthesis and structure-activity optimization of 7-azaindoles containing aza-β-amino acids targeting the influenza PB2 subunit. Eur. J. Med. Chem. 2023, 250, 115185.

[34] Sánchez-Céspedes, J.; Martínez-Aguado, P.; Vega-Holm, M.;Serna-Gallego, A.; Candela, J. I.; Marrugal-Lorenzo, J. A.; Pachón, J.; Iglesias-Guerra, F.; Vega-Pérez, J. M. New 4-Acyl-1-phenylaminocarbonyl-2-phenylpiperazine Derivatives as Potential Inhibitors of Adenovirus Infection. Synthesis, Biological Evaluation, and Structure–activity Relationships. J. Med. Chem. 2016, 59, 5432-5448.

[35] Mazzotta, S.; Marrugal-Lorenzo, J. A.; Vega-Holm, M.; Serna-Gallego, A.; Álvarez-Vidal, J.; Berastegui-Cabrera, J.; Pérez del Palacio, J.; Díaz, C.; Aiello, F.; Pachón, J.; Iglesias-Guerra, F.; Vega-Pérez, J. M.; Sánchez-Céspedes, J. Optimization of piperazine-derived ureas privileged structures for effective antiadenovirus agents. Eur. J. Med. Chem. 2020, 185, 111840.

[36] Nagalakshmamma, V.; Venkataswamy, M.; Pasala, C.; Umamaheswari, A.; Thyagaraju, K.; Nagaraju, C.; Venkata, P. V. Design, synthesis, anti-tobacco mosaic viral and molecule docking simulations of urea/thiourea derivatives of 2-(piperazine-1-yl)-pyrimidine and 1-(4-Fluoro/4-Chloro phenyl)-piperazine and 1-(4-Chloro phenyl)-piperazine – A study. Bioorganic Chemistry, 2020, 102, 104084.

[37] Credille, C. V.; Yao Chen, Y.; Seth M. Cohen. Fragment-Based Identification of Influenza Endonuclease Inhibitors. J. Med. Chem. 2016, 59, 6444–6454.

[38] Kleandrova, V. V.; Speck-Planche, A. The urgent need for pan-antiviral agents: from multitarget discovery to multiscale design. Future Med. Chem., 2020, E 10.4155/fmc-2020-0134 C 2020 Newlands Press -pub. doi.org/10.4155/fmc-2020-0134

[39] Schumann, S.; Kaiser, A.; Nicoletti, F.; Mangano, K.; Fagone, P.; van Wijk, E.; Yan, Y.; Schulz, P.; Ludescher, B.; Niedermaier, M.; von Wegerer, J.; Rauch, P.; Setz, C.; Schubert, U.; Brysch, W. Immune-Modulating Drug MP1032 with SARS-CoV-2 Antiviral Activity In Vitro: A potential Multi-Target Approach for Prevention and Early Intervention Treatment of COVID-19. Int. J. Mol. Sci. 2020, 21, 8803; doi:10.3390/ijms21228803

[40] Konaklieva, M.I.; Plotkin, B.J. Utilization of Existing Human Kinase Inhibitors as Scaffolds in the Development of New Antimicrobials. Antibiotics 2023, 12, 1418.

[41] Maginnis, M. S. β-arrestins and G protein-coupled receptor kinases in viral entry: A graphical review. Cell Signal. 2023, 102, 110558. doi: 10.1016/j.cellsig.2022.110558.

[42] Ni, Z.; Wang, J.; Yu, X.; Ni, Z.; Wang, J.; Yu, X.; Wang, Y; Wang, J.; He, X.; Li, C.; Deng, G.; Shi, J.; Kong, H.; Jiang, Y.; Chen, P.; Zeng, X.; Tian, G.; Chen, H.; Bu, Z. Influenza virus uses mGluR2 as an endocytic receptor to enter cells. Nat Microbiol 2024, 9, 1764–1777.

[43] Orr-Burks, N.; Murray, J.; Todd, K. V.; Bakre, A.; Tripp, R. A. G-Protein-Coupled Receptor and Ion Channel Genes Used by Influenza Virus for Replication. J. Virol. 2021, 95, 1128/jvi.02410-20.

[44] Nagesh, P. T.; Husain, M. Influenza A Virus Dysregulates Host Histone Deacetylase 1 That Inhibits Viral Infection in Lung Epithelial Cells. J Virol. 2016, 90, 4614-4625. doi: 10.1128/JVI.00126-16.

[45] Hussain, M.; Ahmed, F.; Henzeler, B.; Husain, M. Anti-microbial host factor HDAC6 is antagonised by the influenza A virus through host caspases and viral PA. FEBS J 2023, 290, 2744-2759.

[46] Scott, D. E.; Coyne, A. G.; Hudson, S. A.; Abell, C. Fragment-Based Approaches in Drug Discovery and Chemical Biology. Biochemistry 2012, 51, 4990–5003.

## 5. Appendix A

*Compounds' characterization*

Chemical characterization of compounds shown in Table 1:

N-[(2-nitrophenyl)methyl]-N'-pyrimidin-2-ylurea (6a). Bright, yellow crystalline solid (174.5 mg, 34.9%). MP 204.76 ◦ C; MS (m/z): 294.9 (M+Na+); ^{1}H NMR (600 MHz, DMSO-d6) δ δ 10.07 (s, 1H), 8.70 (d, J = 4.9 Hz, 1H), 8.31 (s, 1H), 8.03 (dd, J = 8.3, 1.5 Hz, 1H), 7.97 – 7.92 (m, 1H), 7.70 (ddd, J = 8.5, 7.3, 1.6 Hz, 1H), 7.29 (ddd, J = 8.5, 7.3, 1.3 Hz, 1H) 7.00 (dd, J = 8.5, 1.3 Hz, 1H), 6.61 (ddd, J = 8.4, 6.8, 1.3 Hz, 3H); ^{13}C NMR (101 MHz, DMSO-d6) δ 157.83, 154.24, 153.89, 153.59, 135.92, 135.22, 131.90, 125.27, 119.13, 117.29, 115.37; MS (m/z): Anal. Calcd for $C_{12}H_{11}N_5O_3$, 273.25; found, 271.9. IR (cm-1): 1727.09 (C=O). [21].

3-amino-5-(methylsulfanyl)-N-(2-nitrophenyl)-1H-1,2,4-triazole-1-carboxamide (22). Yellow, crystalline solid (144mg, 28.9%). MP 216.14 ◦ C; MS (m/z): 294.29 ; ^{1}H NMR (600 MHz, DMSO-d6) δ 8.31 (s, 1H), δ 7.95 (dd, J = 8.7, 1.6 Hz, 1H), 7.43 – 7.34 (m, 1H), 7.00 (dd, J = 8.5, 1.3 Hz, 1H), 6.64 – 6.58 (m, 1H), 6.00 (s, 1H), 2.39 (s, 3H).; ^{13}C NMR (100 MHz, DMSO-d6) δ 158.44, 148.00, 141.16, 135.99, 125.98, 125.14, 124.52, 120.76, 116.78, 16.40. MS (m/z): Anal. Calcd for $C_{10}H_{10}N_6O_3S$, 294.29; found, NT. IR (cm-1): 1727.08 (C=O).

3-amino-N-[(2-chlorophenyl)methyl]-5-(methylsulfanyl)-4H-1,2,4-triazole-4-carboxamide (23). Tan, crystalline solid (933 mg, 81.5%). MP 120.98 ◦ C; ^{1}H NMR (600 MHz, DMSO-d6) δ 8.64 (t, J = 6.2 Hz, 2H), 7.45 (d, J = 1.0 Hz, 2H), 7.45 – 7.39 (m, 2H), 6.03 (s, 1H), 4.29 (d, J = 6.0 Hz, 2H), 2.39 (s, 3H); ^{13}C NMR (100 MHz, DMSO-d6) δ 163.35, 151.22, 136.25, 132.19, 129.53, 129.06, 128.79, 127.62, 41.21, 13.66; MS (m/z): Anal. Calcd for $C_{11}H_{12}ClN_5OS$, 297.76, 299.21; IR (cm-1): 1722.38 (C=O).

Ethyl-4-(2-((2-fluorophenyl)sulfinyl)-4-oxoazetidine-1-carboxamido)butanoate (28). Colorless liquid. MS (m/z): 369.10; ^{1}H NMR (81 MHz, CDCl₃) δ 7.97 – 6.94 (m, 4H), 6.57 – 6.20 (m, 1H), 5.54 – 4.94 (m, 1H), 4.13 (q, J = 7.1 Hz, 2H), 3.65 – 2.95 (m, 3H), 2.76 (dd, J = 16.0, 5.2 Hz, 1H), 2.30 (td, J = 7.0, 2.7 Hz, 2H), 1.96 – 1.38 (m, 2H), 1.26 (t, J = 7.1 Hz, 3H).

N-benzyl-2-oxo-4-((3-(trifluoromethyl)phenyl)thio)azetidine-1-carboxamide (30). The product was purified by flash chromatography on silica gel (hexanes: EtOAc, 1:1; v/v) to afford the compound as a viscous oil in 68% yield. ^{1}H NMR (400 MHz, CDCl$_3$): δ 7.77 (1H, m), 7.74 (1H, ddd, J = 1.6, 1.8, 7.9), 7.54 (2H, ddd, J = 1.0, 7.7, 7.9), 7.18-7.29 (2H, m), 6.72 (1H, br, s), 5.26 (1H, dd, J = 2.3, 4.9), 4.41 (1H, dd, J = 0.7, 15.0 ), 3.41 (1H, dd, J = 7.5, 16.0), 2.82 (1H, dd, J = 7.5, 16.0); ^{13}C NMR (125 MHz, CDCl$_3$) δ 165.20, 149.71, 137.79, 137.74, 132.13, 44.57, 131.74 (1C, q, J = 0.32), 131.14, 129.88, 128.95, 127.88, 127.85, 125.90, 57.21, 43.91; IR (neat) υmax (C=O) 1777, 1706 cm-1; Anal. calcd for C18H15F3N2O2S; C, 56.84; H, 3.97; N, 7.36; Found: C, 57.01; H, 4.02; N, 7.46.

1-(2-fluoro-6-hydroxyphenyl)-3-(pyrimidin-2-yl)urea (19). Howard et al. Journal of the American Pharmaceutical Association (1912), 1954, vol. 43, p. 628-630.

N-(2-nitrophenyl)-4-(pyrimidin-2-yl)piperazine-1-carboxamide (20). National Center for Biotechnology Information (2025). PubChem Compound Summary for CID 121589071, N-(2-chloro-5-methoxyphenyl)-4-pyrimidin-2-ylpiperazine-1-carboxamide.RetrievedFebruary21,2025
from https://pubchem.ncbi.nlm.nih.gov/compound/121589071.

N-(2-chloro-5-methoxyphenyl)-4-(pyrimidin-2-yl)piperazine-1-carboxamide (21).

N1-(2-chloro-5-methoxyphenyl)-N4-(2-nitrophenyl)piperazine-1,4-dicarboxamide (22).

1,3-Diazines with platelet-derived growth factor receptor inhibitory activity. Current Patent Assignee: Kyowa Hakko Kogyo Co., Ltd. - US6169088, 2001, A Patent Family Members: CA2239227 A1; WO1998/14431 A1; AU4470897 A; EP882717 A1; CN1208404 A.

N-(2-cyanophenyl)-3-((2,4-difluorophenyl)thio)propenamide (36). National Center for Biotechnology Information (2025).PubChem Compound Summary for CID 18268963, N-(2-cyanophenyl)-3-(2,4-difluorophenyl)sulfanylpropanamide.RetrievedFebruary21,2025
from https://pubchem.ncbi.nlm.nih.gov/compound/18268963.

N-(2-cyanophenyl)-3-((2-(trifluoromethyl)phenyl)thio)propenamide (38). Current Patent Assignee: MEDEIA THERAPEUTICS - WO2013/104829, 2013, A1

N-(2-cyanophenyl)-3-((2-(trifluoromethyl)phenyl)sulfinyl)propenamide (41). National Center for Biotechnology Information (2025). PubChem Compound Summary for CID 70837086, N-[4-cyano-3-(trifluoromethyl)phenyl]-3-(4-fluorophenyl)sulfinylpropanamide.RetrievedFebruary21,2025
from https://pubchem.ncbi.nlm.nih.gov/compound/70837086.